

SPECTRAL ENERGY DISTRIBUTIONS OF INFALLING ENVELOPES

Nuria Calvet ¹

Five College Astronomy Department, University of Massachusetts,
526 LGRB, Amherst, MA 01003, USA

RESUMEN

Aunque el colapso de una nube inicialmente esférica puede explicar la distribución espectral de energía (DEE) de las fuentes con espectro plano inmersas en la nube de Tauro, encontramos que si las envolturas de material tienen cavidades amplias, como las que se necesitan para explicar las imágenes que se observan de esas fuentes, entonces la DEE no puede reproducirse. Además, el material debería estar rotando demasiado rápidamente. Por todo ello, presentamos un modelo alternativo que elimina esas discrepancias, partiendo de un colapso iniciándose con una distribución de material plana. Con este modelo, pueden explicarse consistentemente tanto las DEEs, como las imágenes que se observan. Dada la distribución intrínseca achatada del material, no se necesita que éste rote rápidamente. Se presenta un test de este modelo realizado con HL Tau.

ABSTRACT

Even though the collapse of a slowly rotating spherical cloud can explain the fluxes of embedded and flat-spectrum sources in the Taurus cloud, we discuss the problems presented by this model: namely, extremely large rotational rates and inconsistency between the large cavities required to explain the images and the need of having enough hot envelope material to produce near and mid infrared fluxes. As an alternative model, we propose that the collapse starts from a sheet of material, in which case the flattening is geometrical and always present, polar cavities naturally appear, explaining observed images, and there is enough hot material near the star to reproduce observed fluxes. As a test case, fluxes and images for HL Tau are presented.

Key words: ISM: DUST, EXTINCTION — STARS: PRE-MAIN-SEQUENCE

1. INTRODUCTION

I describe here work done with Lee Hartmann, Scott Kenyon, Barbara Whitney, and Alan Boss on the study of embedded objects in star-forming regions. These objects are characterized by having fluxes in IRAS bands, extended images in the near infrared, and association with jets and optical outflows in most cases. We identified them with protostars, that is, stars in the process of being formed. We had the necessary tools to undertake a complete study of these sources: we had developed radiative transfer codes for extended geometries to obtain spectral energy distributions (SEDs), including self-consistent radiative equilibrium temperature calculations; we had a Monte Carlo code to calculate scattered light images and polarizations; and we had put together an extensive data base for young objects in molecular clouds. So, we felt especially well equipped to study these sources in detail and try to understand their individual and global characteristics.

¹On leave from Centro de Investigaciones de Astronomía CIDA, Mérida, Venezuela

2. COLLAPSE FROM A SPHERICAL CLOUD

We started with the standard model of star formation, that is, the near free-fall collapse of a slowly rotating spherical cloud producing at the center a stellar object surrounded by a disk (Terebey, Shu, & Cassen 1984, TSC hereafter; Shu, Adams, & Lizano 1987). This model had already been tried successfully for a few sources (Adams & Shu 1986; Adams, Shu, & Lada 1987, 1988; Butner et al. 1991; Natta et al. 1992), but we undertook a systematic study of all the embedded sources in the Taurus-Auriga cloud (Kenyon, Calvet, & Hartmann 1993).

For this, we applied standard radiative transfer techniques in spherical geometry to calculate the radiative equilibrium temperature for the angle-averaged density, and a ray-by-ray solution for given inclination i to calculate the flux including the angular dependence of the density. The standard model explained well the observed properties of the Taurus embedded sources. In particular, we found a mean mass infall rate of $\sim 4 \times 10^{-6} M_{\odot} \text{ yr}^{-1}$, assuming a typical mass of $0.5 M_{\odot}$, while the standard model prediction for the temperature of the Taurus molecular cloud, $10^{\circ}K$, is $\sim 2 \times 10^{-6} M_{\odot} \text{ yr}^{-1}$.

To explain the high observed fluxes in the near and mid infrared, we did require large values for the centrifugal radius, $R_c \sim 70 - 300 \text{ AU}$, even for the youngest sources. A large value of R_c implies a large inner region of departure from spherical symmetry, where the density no longer goes as $r^{-3/2}$ but rather as $\sim r^{-1/2}$, which lowers the optical depth towards the hot inner regions, allowing more near and mid-infrared flux to escape. This result indicated that a large degree of flattening was required from very early times in the evolution of the system, or, in the context of the model, that cloud rotation rates were large, near the largest observed.

3. FLAT-SPECTRUM SOURCES

We also studied the so called "flat-spectrum" sources, that is, sources for which the SED, λF_{λ} , remains essentially constant over nearly two decades in wavelength. Many attempts have been made in recent years to understand the nature of these sources, but most of these have assumed that the system consists of a disk and a star only, with the infrared flux coming from the disk. As a consequence, the emphasis has been put in obtaining a disk structure that gives fluxes similar to the observed spectra (Adams, Lada, & Shu 1988; Natta 1993). However, the flat spectrum sources have *extended images* in the optical and near infrared; moreover, they have large degree of polarization. These properties imply that some material is present at large distances from the central object, so that rather than modifying standard disk accretion theory, it is simpler to look at the evolution of the infalling envelope in the standard model. The similarity of the SEDs of some of the flat-spectrum sources with those of embedded sources in Taurus (c.f. HL Tau and 04016+2610, Fig. 1 in Calvet et al. 1994) supports the assumption that the envelope may be an essential contributor to the flux in these sources. Calvet et al. 1994 could fit the spectra of several flat-spectrum sources assuming that collapse is still proceeding in these objects so a large fraction of the total flux is emitted by the envelope. This study showed that the flat-spectrum sources are young stars which still have significant infall.

4. CONFRONTATION BETWEEN SED AND IMAGE ANALYSES: THE PROBLEM WITH THE CAVITY

The results of the SED analysis on the properties of the embedded sources in the Taurus cloud (Kenyon, Calvet, & Hartmann 1993) were consistent with those obtained from the fit to the images and known polarization of the sources using Monte-Carlo techniques (Kenyon et al. 1993). A "hole", or region of lower density, is required to explain the observed images (Whitney & Hartmann 1993), and in these studies, a cavity following a streamline, of arbitrary opening angle at infinity, was excavated in the corresponding TSC model. Jets or outflows were claimed to be responsible for carving the holes.

For most of the embedded sources in Taurus, the images are narrow and small opening angle holes are required. However, for some of these sources or for many of the flat-spectrum sources, opening angles of 30° or more are necessary to explain the observations. In fact, the bowl-like cavities at the site of the source seem to be a very common feature (see Reipurth & Cernicharo 1995 in these Proceedings). With cavities of this size in the TSC model, the SEDs could not be reproduced.

Consider that there is a mechanism able to excavate a cavity of large opening angle at infinity. The material at the edge of that cavity is falling towards the central object, and will do so following a streamline. The material will fall retaining its angular momentum, so that the larger the opening angle, the farther out on the equatorial plane the material lands, as shown in Figure 1, left panel. Since the envelope is heated by stellar light, the maximum temperature of the envelope, reached at the landing point of the material at the edge of the cavity,

decreases as the opening angle of the cavity increases. For instance, with an opening angle at infinity of $\sim 30^\circ$, the material closest to the star lands on the equatorial plane at $\sim 15AU$, for an $R_c = 50AU$. For a source luminosity of $5L_\odot$ and typical mass infall rates, temperatures higher than $1000^\circ K$ are attained only inside $0.4 AU$, and higher than $500^\circ K$ only inside $\sim 2AU$. Therefore, for large opening angles, the envelope can only reach a few hundred degrees, producing little near and *mid* infrared flux. Figure 1, right panel, illustrate the effect of cavities of increasing opening angle on the SED.

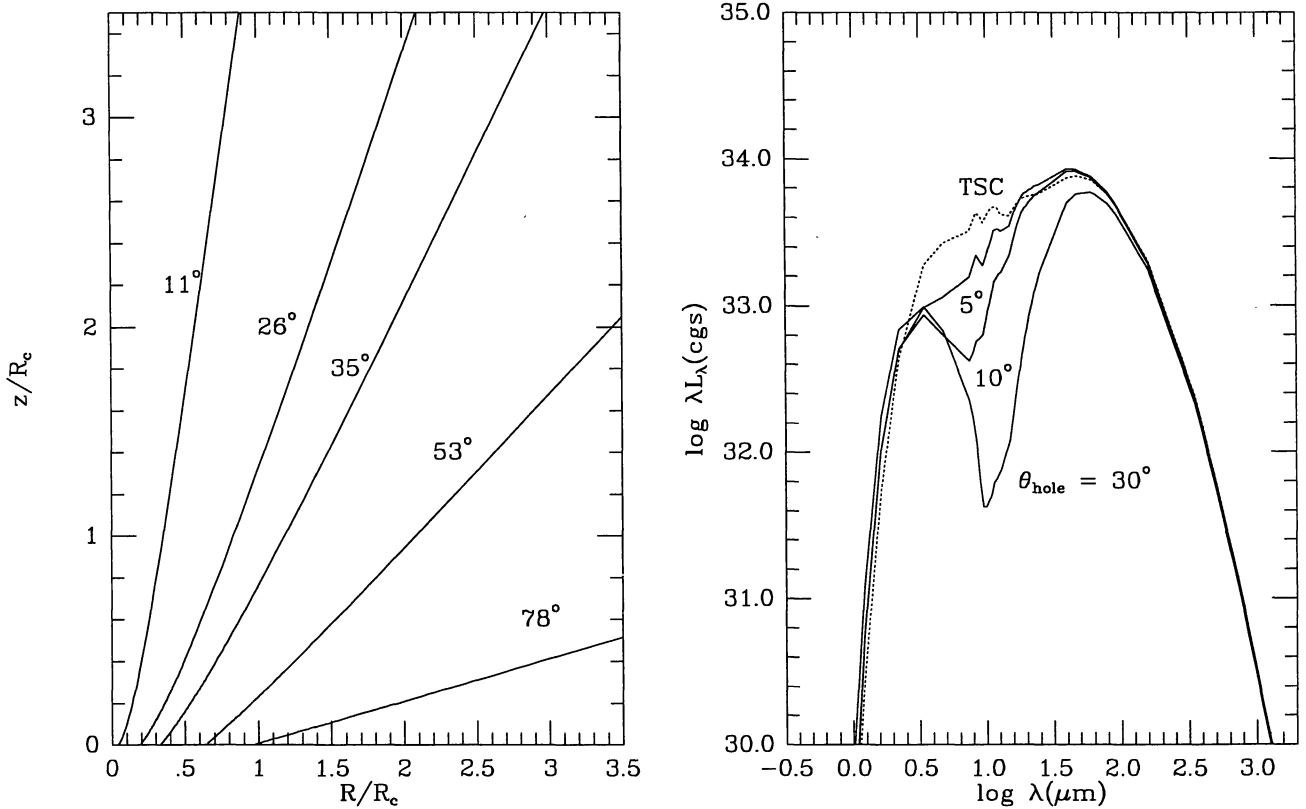


Fig. 1.— Left panel: Streamlines for the TSC model. Curves are labeled by angle at infinity. Right panel: Effects of a cavity of opening angle θ_{hole} on the SED calculated with an TSC model. Model parameters: $L = 5L_\odot$, $\dot{M} = 3 \times 10^{-6} M_\odot \text{ yr}^{-1}$ (if $M = 0.5M_\odot$), $R_c = 100AU$.

5. POSSIBLE RESOLUTION OF THE PROBLEM: SHEET COLLAPSE

One possible way of solving the contradiction stated before is to invoke the presence of non-standard disks. With an appropriate (and arbitrary) exponent of a power law temperature structure, an optically thick disk could produce enough mid-infrared flux to “fill the gap” left by the cool envelope. Alternatively, Galli & Shu (1993a,b) have considered the collapse of an initially spherical cloud permeated by a magnetic field. A flattened structure results from this collapse, which they identify with the elongated structures observed at distances of order $10^3 AU$ or more around forming objects. We prefer to explore a simpler solution, which is supported by observations and other considerations.

Molecular clouds are elongated by a typical 2:1 ratio (Myers et al. 1991). Fragmentation to form multiple systems is better accomplished in sheets or filaments (Larson 1985; Bonnell & Bastien 1992; Bonnell et al. 1994). Following these indications, we considered a collapse from an initial sheet-like structure of material, instead of departing from a spherical cloud. This type of collapse has several advantages:

- the flattening is *intrinsic* to the collapse, from the very earliest stages;

- the flattened collapse naturally produces a “hole”, that is, a polar region of low optical depth *with a large opening angle*; due to the z-dependence of the density of the original hydrostatic cloud:

$$\rho(z) = \rho(0) \operatorname{sech}^2(z/H), \quad (1)$$

where H is the scale height

$$H = c_s^2 / (\pi G \Sigma) \quad (2)$$

with c_s the sound speed and Σ the total surface density, material gets depleted faster at the poles than at the equator. But the material can fall close to the star and *get heated*, because the flattening is not due to rotation.

We performed the hydrodynamic calculation of the collapse of a marginally stable, self-gravitating $1M_\odot$ layer, using the code of Boss & Myhill (1992) (Hartmann et al. 1994). The collapse in this case is not a pure “inside-out” collapse. The whole region, which was chosen to correspond to the critical wavelength for instability of the layer (Spitzer 1978), begins to move at subsonic velocities essentially parallel to the mid-plane. After a time $t \sim 5t_{ff}$, where $t_{ff} = [3\pi/32G\rho(0)]^{1/2} \sim 5 \times 10^4 (n_H(0)/3 \times 10^6 \text{ cm}^{-3}) \text{ yr}$ is the free-fall time to the mid-plane, motions become supersonic, largely radial and a central core begins to develop. By $t \sim 7t_{ff}$, a central core of $0.65M_\odot$ has developed and the mass infall rate has leveled to $\sim 6 \times 10^{-6} M_\odot \text{ yr}^{-1}$, somewhat higher than that for spherical collapse (cf. Hartmann et al. 1994). Figure 2 shows the density isocontours at different times.

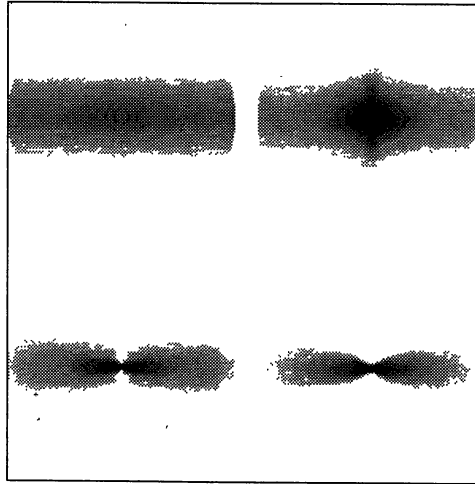


Fig. 2.— Density isocontours for the collapse of a marginally stable sheet. Upper left: $t = 2.7t_{ff}$; upper right: $t = 6t_{ff}$; lower left: $t = 6.5t_{ff}$; and lower right: $t = 7t_{ff}$ (see text).

The main results of these calculations are that the collapse of a self gravitating sheet results in a flattened infalling envelope, with flattening increasing with time; since the polar regions fall in before the equatorial regions, a relatively evacuated “polar hole” naturally forms. No additional mechanisms are required to open the hole, which intrinsically has large opening angles. In addition, since the flattening is not due to rotation, but is intrinsic to the collapse, the rotation rates of the original clouds need not be as high as required by the TSC model.

6. THE SHEET COLLAPSE WITH ROTATION: APPROXIMATE ANALYTICAL MODEL

We can obtain an approximate expression for the density at a given time assuming that we have a free-fall collapse from an initially flattened, slowly rotating layer towards a central point mass, which would be adequate after the collapse has proceeded for some time. With this assumption, we obtain

$$\rho(r, \mu) = \rho_{TSC}(r, \mu) \operatorname{sech}^2(\eta\mu_0) [\eta/\tanh(\eta)], \quad (3)$$

where ρ_{TSC} is the TSC density distribution for a given \dot{M} and R_c , at radius r and angle θ , such that $\mu = \cos \theta$ and $\mu_0 = \cos \theta_0$. The parameter η is given by

$$\eta = r_0/H = (t/t_H)^{2/3} \quad (4)$$

where $r_0(t)$ is the radius where the material reaching the midplane at time t came from, and t_H is the free-fall time from H . This parameter introduces an additional angular dependence on the TSC density distribution, increasing the polar evacuation. In addition, η increases with time, so that if we define the “opening angle” of the evacuated region as given by $\mu_0 = 1/\eta$, then we can see that the polar “hole” becomes wider as the system evolves.

Using the η expression for the density, eqn. (3), and a non-spherical radiative equilibrium temperature distribution, we have calculated SEDs for values of the mass infall rate similar to the typical value obtained from the spherical collapse analysis applied to the Taurus sources. The general feature of the SEDs in this model is that they are similar to the TSC SEDs, but the parameter η , that is, the degree of geometrical flattening, plays the same role as R_c did. In the TSC model, as R_c increased, the SEDs widened up, showing more of the central object at short wavelengths. In the sheet-collapse models, the SEDs widen up as η increases. Therefore, for a given SED, a smaller value of original rotation is required for similar value of the mass infall rate.

In Figure 3, we compare models with $\eta = 2, i = 30^\circ$ and $\eta = 3, i = 60^\circ$ with the observed SED of HL Tau. As before, the mass infall rate is $\sim 4 \times 10^{-6} M_\odot \text{ yr}^{-1}$, but $R_c = 50 \text{ AU}$. A standard accretion disk of half the total luminosity shows in the near infrared in these models. The agreement is particularly good, especially considering that the models were not explicitly constructed to fit HL Tau.

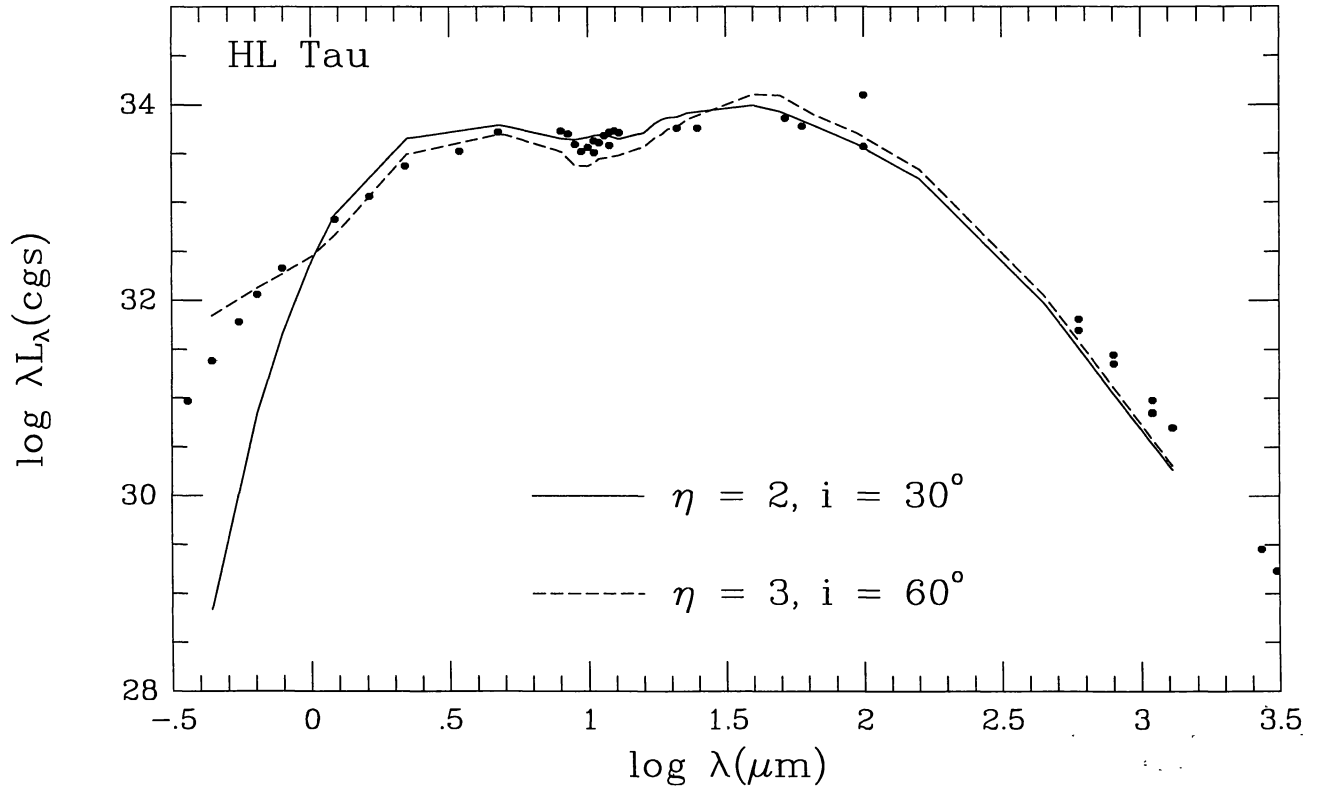


Fig. 3.— Comparison of sheet-collapse models with HL Tau fluxes. Parameters for the models are $L = 5L_\odot$, $\dot{M} = 3 \times 10^{-6} M_\odot \text{ yr}^{-1}$, $R_c = 50 \text{ AU}$, and $\eta = 2, i = 30^\circ$ and $\eta = 3, i = 60^\circ$.

B. Whitney has kindly calculated scattered light images for models with standard TSC parameters for Taurus and various values of η . These calculations are shown in Figure 4 for the J band. The opening angle of the images increases with increasing η , and it is interesting that values of η between 2 and 3 also give images

similar to those of HL Tau (Mundt et al. 1990). In addition, the envelope density contours for $\eta \sim 2 - 3$ are similar to those shown in the lower left panel of Fig. 2, in agreement with the claim of Hayashi et al. (1993) that HL Tau can be explained by an infalling *disk*.

Moreover, the scattering calculations indicate that the images show the *structure of the flattened infall*, explaining the universal character of the bowl-like shape.

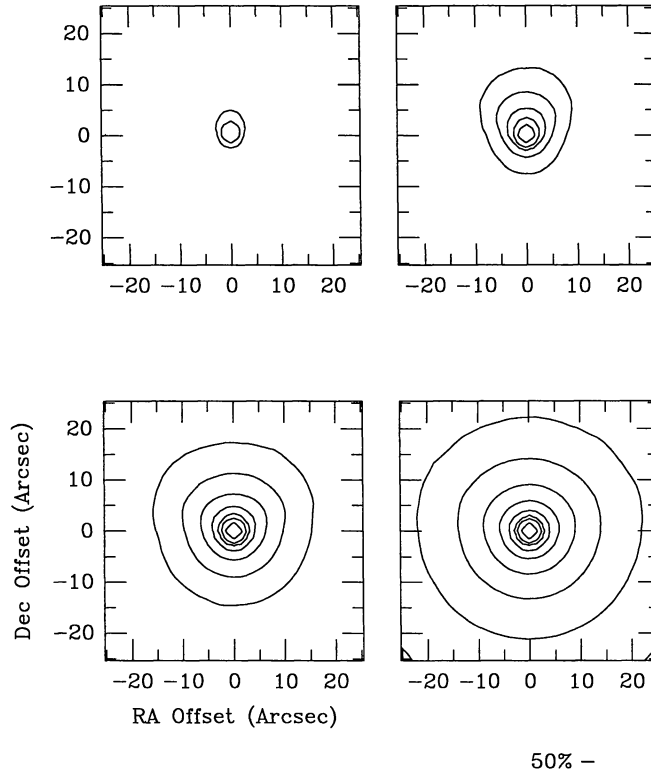


Fig. 4.— Scattered light images for various values of η . Parameters are the standard for the Taurus cloud. Models calculated at $J, i = 60^\circ$. Upper left: $\eta = 1$; upper right: $\eta = 2$; lower left: $\eta = 3$; and lower right: $\eta = 4$. (Calculations by B. Whitney.)

7. SUMMARY AND CONCLUSIONS

The collapse from a slowly rotating spherical cloud can explain the SEDs of deeply embedded and flat spectrum sources in Taurus, although large rotational rates are required to explain the flattening. In addition, if the spherical infalling regions had cavities with opening angles as big as 30° or more, as the analyses of the scattered light images suggest, then the model would fail to explain the observed SED. We propose as a solution to this impasse that the collapse starts from a sheet-like structure. In this case, the flattening is intrinsic to the collapse and evacuated polar regions result from the geometry. As a test case, we have calculated SED and scattered light images for HL Tau and have found that the results provided by these independent analyses are consistent and give good fits to the observations. The images show the structure of the flattened infall.

I am very grateful to the Instituto de Astronomía of the Universidad Nacional Autónoma de México for the financial support they gave me. I would like to thank B. Whitney for providing me with the calculation of scattered light images for the η models.

REFERENCES

Adams, F. C., & Shu, F. H. 1986, *ApJ*, 308, 836
Adams, F. C., Lada, C. J., & Shu, F. H. 1987, *ApJ*, 312, 788
Adams, F. C., Lada, C. J., & Shu, F. H. 1988, *ApJ*, 326, 865
Bonnell, I., Arcoragi, J. P., Martel, H., & Bastien, P. 1992, *ApJ*, 400, 579
Bonnell, I., & Bastien, P. 1992, *ApJ*, 401, 654
Boss, A. P., & Myhill, E. A. 1992, *ApJS*, 83, 311
Butner, H. M., Evans, J. J., II, Lester, D. F., Levreault, R. M., & Strom, S. E. 1991, *ApJ*, 376, 636
Calvet, N., Hartmann, L., Kenyon, S., & Whitney, B. 1994, *ApJ*, 434, 330
Cassen, P., & Moosman, A. 1981, *Icarus*, 48, 353
Galli, D., & Shu, F. H. 1993a, *ApJ*, 417, 220
Galli, D., & Shu, F. H. 1993b, *ApJ*, 417, 243
Hartmann, L., Boss, A., Calvet, N., & Whitney, B. 1994, *ApJ*, 430, L49
Hayashi, M., Ohashi, N., & Miyama, S. 1993, *ApJ*, 418, L71
Kenyon, S. J., Calvet, N., & Hartmann, L. 1993, *ApJ*, 414, 676
Kenyon, S. J., Whitney, B., Gómez, M., & Hartmann, L. 1993, *ApJ*, 414, 773
Larson, R. B. 1985, *MNRAS*, 214, 379
Mundt, R., Ray, T. P., Bührke, T., Raga, A. C., & Solf, J. 1990, *A&A*, 232, 37
Myers, P. C., Fuller, G. A., Goodman, A. A., & Benson, P. J. 1991, *ApJ*, 376, 561
Natta, A., Palla, F., Butner, H. M., Evans, J. J., II, & Harvey, P. M. 1992, *ApJ*, 391, 805
Natta, A. 1993, *ApJ*, 412, 767
Reipurth, B., & Cernicharo, J. 1995, in *Disk, Outflows and Star Formation*, ed. S. Lizano & J. M. Torrelles, RevMexAASC, 1, 43
Shu, F. H., Adams, F. C., & Lizano, S. 1987, *ARA&A*, 25, 23
Spitzer, L., 1978, *Physical Processes in the Interstellar Medium* (New York: J. Wiley), 283
Terebey, S., Shu, F. H., & Cassen, P. 1984, *ApJ*, 286, 529
Whitney, B. A., & Hartmann, L. 1993, *ApJ*, 402, 605